Heliyon 5 (2019) e02123

Contents lists available at ScienceDirect

Heliyon

journal homepage: www.heliyon.com

Heliyon

CAD/CAM splint and surgical navigation allows accurate maxillary segment positioning in Le Fort I osteotomy

Tatsuo Shirota [a,*], Sunao Shiogama [a], Yusuke Asama [b], Motohiro Tanaka [a], Yuji Kurihara [a], Hiroshi Ogura [c], Takaaki Kamatani [a]

[a] *Department of Oral and Maxillofacial Surgery, School of Dentistry, Showa University, Tokyo, Japan*
[b] *Department of Orthodontics, School of Dentistry, Showa University, Tokyo, Japan*
[c] *Department of Information Science, Faculty of Arts and Sciences at Fujiyoshida, Showa University, Fujiyoshida, Japan*

ARTICLE INFO

Keywords:
Surgery
CAD/CAM splint
Surgical navigation
Orthognathic surgery
Surgical simulation

ABSTRACT

Purpose: To evaluate the accuracy of the maxillary segment positioning method using a splint fabricated by computer-aided design/computer-aided manufacturing (CAD/CAM) and surgical navigation in patients who required two-jaw surgery.
Methods: Subjects were 35 patients requiring two-jaw surgery. A 3-dimensional (3D) skull model was prepared using cone-beam computed tomography (CBCT) data and dentition model scan data. Two-jaw surgery was simulated using this model, and a splint for maxillary positioning was fabricated by CAD/CAM. Using coordinate transformation software, the coordinate axis of surgical simulation data was merged with the navigation system, and data were imported to the navigation system. The maxillary segment was placed using the CAD/CAM splint, and consistency of the maxillary segment position with that planned by simulation was confirmed using the navigation system. CBCT taken at 4 weeks postoperatively and the prediction image fabricated using surgical simulation were superimposed. Predicted movement distances (PMD) at 6 arbitrary measurement points and actual movement distance (AMD) in surgery were measured. Differences of 3D measurements between the surgical simulation and postoperative results were evaluated.
Results: No significant differences were seen between PMD and AMD at most measurement points on the X and Y axes. Although significant differences between PMD and AMD were seen on the Z axis, no difference was evident between linear distance on the estimated image and postoperative CBCT image at most measurement points in 3D space. Mean error at measurement points between the PMD and AMD ranged from 0.57 mm to 0.78 mm on the X axis, 0.64 mm–1.03 mm on the Y axis, and 0.84 mm–0.90 mm in the Z axis.
Conclusion: Position of the maxillary segment moved by the CAD/CAM splint in Le Fort I osteotomy was almost consistent with the position established by simulation using the navigation system, confirming clinical accuracy.

1. Introduction

In orthognathic surgery, both acquisition of stable occlusion and balanced maxillofacial morphology are important. Restoring balance to a deformed facial morphology requires alignment of the maxillary and facial midlines. Anteroposterior inclination of the occlusal plane also affects the mental position, and lateral inclination affects facial symmetry. Accordingly, maxillary repositioning is a very important process in two-jaw surgery, because of the influence on postoperative facial morphology. The maxillary segment has to be placed as planned and fixed at an accurate position. In the previous maxillary repositioning method employed in Le Fort I osteotomy, an intermediate surgical splint for maxilla repositioning was generally prepared in model surgery before the actual surgery, the anteroposterior and lateral positions of the maxillary segment were decided by setting the baseline to the mandible, and the maxilla was repositioned by measuring only the vertical position [1].

There have been reports on using CAD/CAM splints designed by simulation software for orthognathic surgery and fabricated using rapid prototyping technology as intermediate splints for maxillary repositioning to accurately reflect the virtual surgical planning results during the actual surgery [2, 3, 4, 5, 6]. However, there is no definitive evidence

* Corresponding author.
E-mail address: tshirota@dent.showa-u.ac.jp (T. Shirota).

https://doi.org/10.1016/j.heliyon.2019.e02123
Received 30 January 2019; Received in revised form 24 April 2019; Accepted 18 July 2019

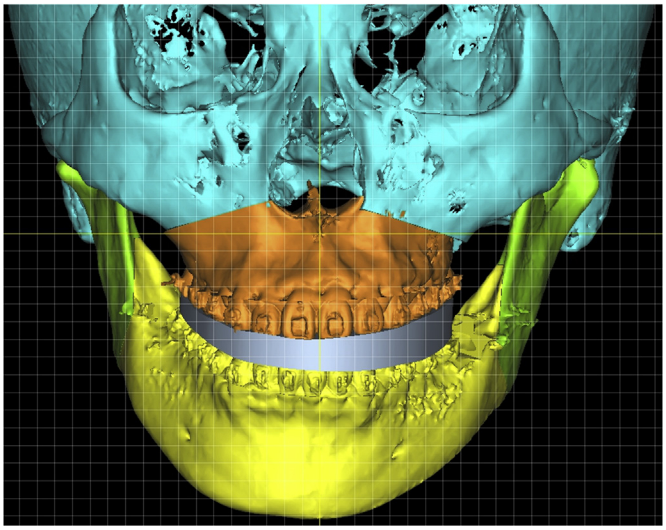

Fig. 1. Design of the CAD/CAM splint: CBCT data acquired using a simulation system (ProPlan CMF version 3.0) designed exclusively for maxillofacial surgery and dentition model-scanning data are integrated, and a 3D skeletal model of the head with reproduced dentition morphology is prepared. Using this model, the Le Fort I osteotomy line is drawn and surgical simulation of maxillary movement is performed, and an intermediate splint for maxillary positioning is designed. A splint is prepared from this data using a 3D printer.

that maxillary repositioning using CAD/CAM splints is more accurate than that using the conventional method. Maxillary repositioning is influenced by the accuracy of the intermediate and perioperative position of the mandibular condyle in the temporalis fossa [7]. As temporomandibular joint movement is unstable under general anesthesia, the double splint method, with which the maxillary position is determined based on the mandibular position, may lead to an inaccurate maxillary position [6]. If maxillary repositioning is performed referencing the unstable mandibular position, it is considered difficult to determine the position that accurately reflects the simulation results even using the CAD/CAM splint designed by surgical simulation software. The present study was performed based on the hypothesis that accurate repositioning is possible by confirming the maxillary position guided by the CAD/CAM splint in real time.

The purpose of this study was to evaluate the accuracy of the maxillary segment positioning method in patients requiring two-jaw surgery by integration of surgical simulation, CAD/CAM sprint, and intra-operative control using a real-time navigation system.

2. Methods

2.1. Subjects

Participants in this study were 35 patients who required two-jaw surgery comprising Le Fort I osteotomy and bilateral sagittal split osteotomy (BSSRO) at our university hospital between August 2017 and March 2018. Informed consent was obtained for both the treatment plan and surgical method. Patients with a dental implant or crown prosthesis on the upper teeth were excluded. All patients provided informed consent to the treatment strategy and surgical procedure and this study was performed after approval by the medical ethics committee of the School of Dentistry at Showa University (DH2017-005). All surgeries were performed by the same surgeon.

2.2. Acquisition of skeletal data using cone-beam computed tomography (CBCT)

Upper and lower dentition models were prepared 14 days before surgery. A 1.5-mm thick plastic plate (DURAN®; SCHEFU-DENTAL, Am Burgberg, Germany) was pressure-welded to the upper dentition model to prepare the splint. Self-curing resin with contrast-enhancing properties (Bone Shade Resin CT350; Yamahachi Dental, Gamagori, Japan) was added to the labial side of the splint, and a splint with 5 randomly set

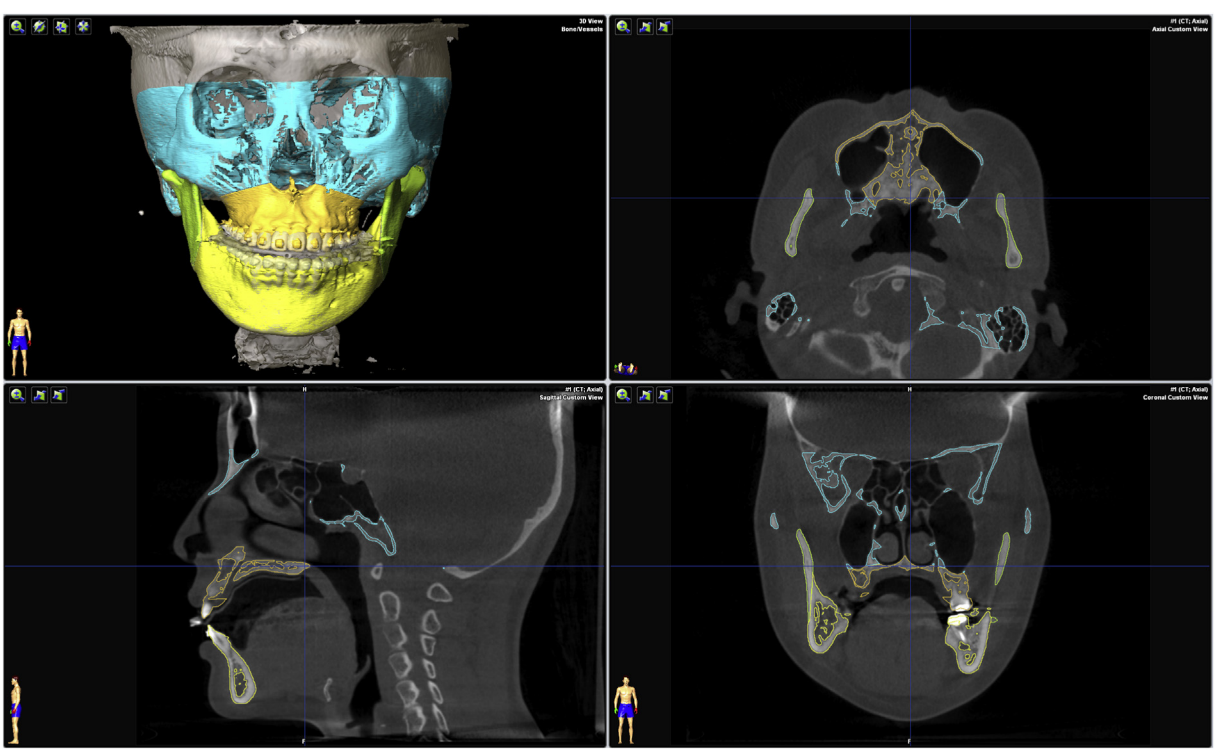

Fig. 2. Superimposition of the object of surgical simulation with the CT image on iPlan CMF 3.0: When coordinate-transformed surgical simulation data are imported to iPlan CMF 3.0, the object of surgical simulation is able to be accurately superimposed with the iPlan CMF 3.0 CT image.

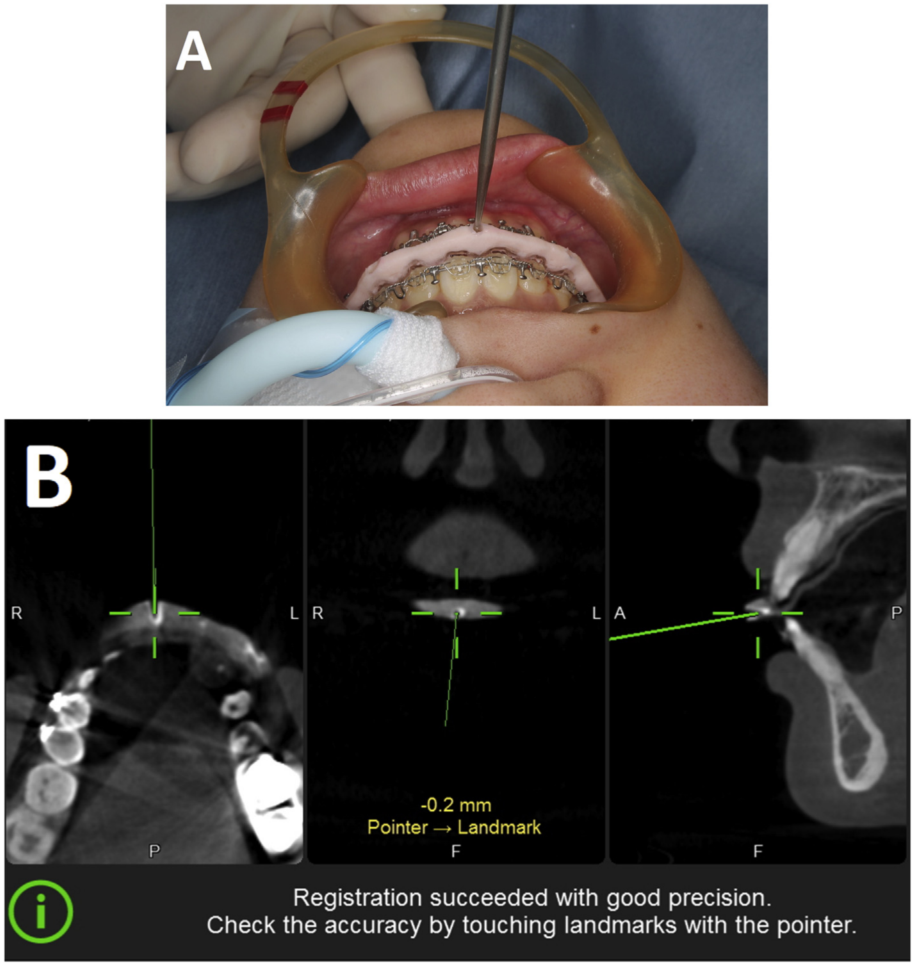

Fig. 3. Registration using a splint with references: Consistency is confirmed between positions in the oral cavity indicated by the navigation pointer (A) and positions on the CT image (B).

reference points was prepared. CBCT images were acquired in a state of centric occlusion with this splint and references using an X-ray CBCT device (KaVo 3D eXam; KaVo Dental Systems Japan, Yao, Japan) under the following acquisition conditions: tube voltage, 120 kV tube current, 5 mA; and slice thickness, 0.25 mm. The acquired data were stored in the Digital Imaging and Communications in Medicine (DICOM) format.

2.3. Acquisition of dentition information using a laser scanner

Plaster upper and lower dentition models prepared 14 days before surgery were scanned using a laser scanner (KaVo ARCTICA Scan; KaVo Dental Systems Japan) and stored as Standard Triangulated Language (STL) data.

2.4. Preoperative simulation and design of the CAD/CAM splint

DICOM data from CBCT acquired preoperatively were imported to simulation software designed specifically for maxillofacial surgery (ProPlan CMF version 3.0; Materialize, Tokyo, Japan) and converted to STL data. STL data for upper and lower dentition models were imported to ProPlan CMF version 3.0 software, integrated with CBCT image data, and a 3-dimensional (3D) skull model accurately reproducing the dentition morphology was prepared. Using this skull model, an osteotomy line for Le Fort I osteotomy was set, maxillary placement was simulated, and an intermediate splint for maxilla repositioning was designed in which the osteotomy line, direction of movement of the maxillary segment, and amount of movement were set referring to the results of cephalometric analysis (Fig. 1). Data for the intermediate splint designed on the simulation software were output into a 3D printer (ULTRA3SP; Envision TEC, Gladbeck, Germany) and the splint was prepared. In addition, to predict the amount of bone removal accompanying movement of the mandible and skeletal morphology, the mobile mandible was placed referring to the results of cephalometric analysis and model surgery. From the surgical simulation data, an object with incision line settings for Le Fort I osteotomy and BSSRO, and an object in which the jaw bones were divided following the incision lines and each bone segment was moved to the planned position were prepared and individually stored as STL data in ProPlan CMF version 3.0.

2.5. Import of STL data for surgical simulation into the navigation system

The navigation system used in this study was an optical navigation system (KICK® Navigation System; BRAINLAB, Munich, Germany). DICOM data for the CBCT acquired before surgery were imported into simulation software designed exclusively for this system (iPlan CMF 3.0, BRAINLAB) and converted to STL data, and a craniofacial bone object was prepared. To use the object of the surgical simulation prepared using ProPlan CMF version 3.0 in the navigation system, it was necessary to import this simulation object into iPlan CMF 3.0 and superimpose it over the craniofacial bone object prepared on iPlan CMF 3.0. However, if an object prepared on ProPlan CMF version 3.0 is directly imported to iPlan CMF 3.0, the imported object is rotated 180° around the coronal plane. Thus, STL data from the surgical simulation were first opened in coordinate transformation software (3-matic Medical 12.0ST; Materialize,

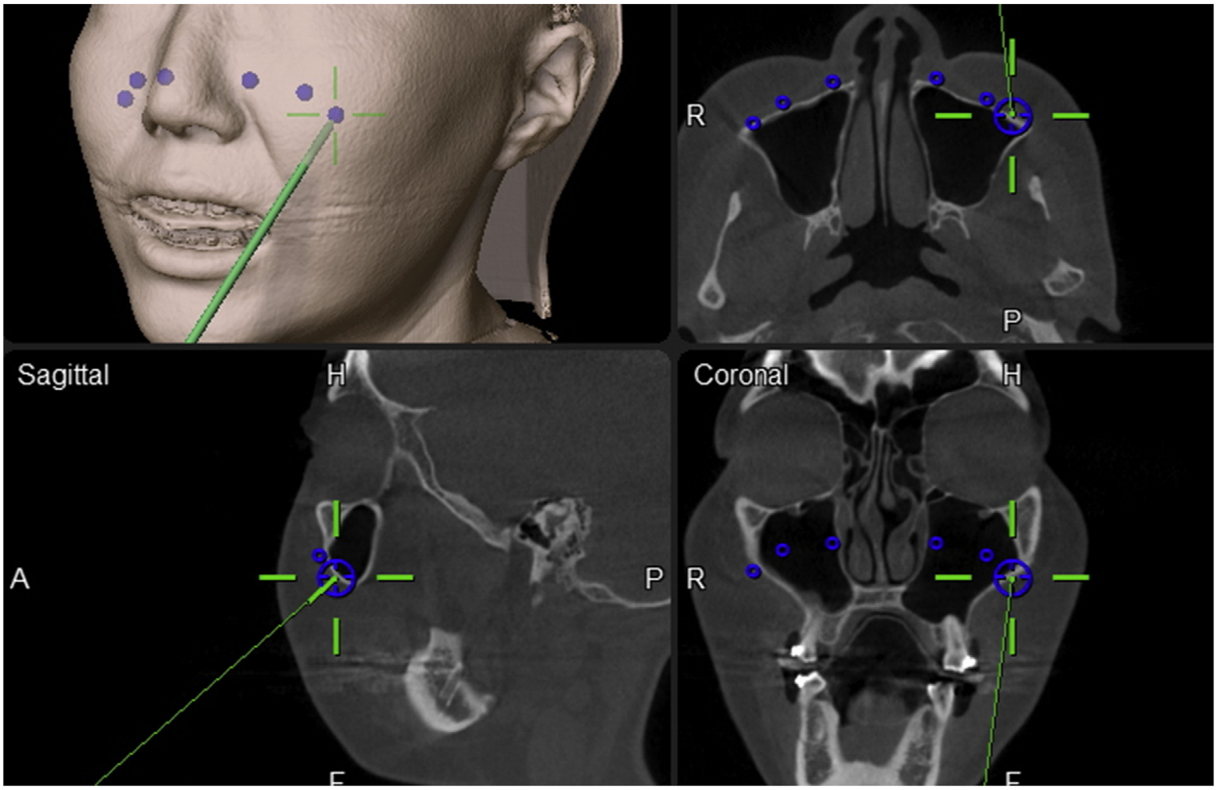

Fig. 4. Switching to intraoperative landmark-based registration: To perform re-registration after mobilization of the maxilla, 6 points are set on the maxillary surface at sites superior to the osteotomy line using a round bar (diameter, 1 mm) and registered as intraoperative landmarks. Splint-based registration is then switched to landmark-based registration.

Tokyo, Japan) and the coordinate axes were merged with those of iPlan CMF 3.0. Surgical simulation data converted to these coordinates were sent to iPlan CMF 3.0, enabling accurate superimposition of the objects of surgical simulation with the CT image on iPlan CMF 3.0 (Fig. 2). Superimposed data were imported to the navigation system and used during the actual surgery.

2.6. Registration for navigation

Under general anesthesia, a head band was attached to the patient to set a reference antenna, followed by attachment of the splint with references used for acquisition of the CBCT image and registration to match the CBCT data with the intraoperative position information (Fig. 3).

During the Le Fort I osteotomy, the maxillary surface was exposed using the standard method and an osteotomy line was drawn on the maxilla surface while indicating the points coinciding with the simulated osteotomy line with a pointer probe displayed on the navigation system screen. To enable re-registration after mobilization of the maxilla, 6 points were set on the maxilla surface superior to the osteotomy line and registered as intraoperative landmarks. This registration was switched from that based on the splint to that based on the landmarks (Fig. 4). The accuracy of navigation was confirmed periodically during surgery and was maintained by repeating landmark-based registration as needed.

2.7. Navigation-assisted Le Fort I osteotomy

Using tracker-equipped Piezosurgery Medical Technology, Carasco, Italy), osteotomy was performed following the osteotomy line drawn on the maxillary surface. The lateral wall of the nasal cavity was processed by osteotomy using Piezosurgery and a bone chisel, and the maxillary segment was mobilized. To place the mobile maxillary segment to the planned position, inter-maxillary fixation was applied through the CAD/CAM-fabricated intermediate splint. A postoperative image was displayed on the screen of the navigation system to confirm the position of the maxillary segment. The positions of orthodontic brackets in the upper central incisor, canine, and first molar were indicated with a pointer, and whether these points coincided with the simulation image was confirmed. When positions of the two images did not match, the maxillary segment was adjusted by removing interfering bone until a match with the simulation image was obtained (Fig. 5). The position was repeatedly assessed until the two images matched, after which the maxillary segment was fixed with a titanium mini plate (Matrix-ORTHOGNATHIC JAPAN System; Johnson & Johnson, Tokyo, Japan). After fixation of the maxillary segment, BSSRO was performed. The mobile mandibular segment was fixed with a titanium mini-plate (MatrixORTHOGNATHIC JAPAN System) through the final splint following the standard BSSRO intermaxillary fixation method.

2.8. Post-operative analysis

The iPlan CMF 3.0 displays the reference points setting the base point at the center of the incorporated DICOM data, and the distance of a specific position from the base point on the CBCT image can be presented on the X axis (horizontal direction), Y axis (anteroposterior direction), and Z axis (vertical direction). Distances from the base point on the right, anterior, and upper directions were regarded as positive on the X, Y, and Z axis, respectively, and presented in millimeters. Using the function to superimpose pre- and postoperative data under a software algorithm, termed image fusion, equipped in iPlan CMF 3.0, CBCT DICOM data acquired 1 month after surgery were superimposed onto the post-operative 3D skeletal image of the head, setting the baseline to the pre-operative 3D skeletal image, in which the base point of the superimposition was distributed 3-dimensionally as several points. As there was no change in positions other than the maxillary segment in the superimposition referring to these base points, the 2 images could be compared based on measured values. Using this procedure, a

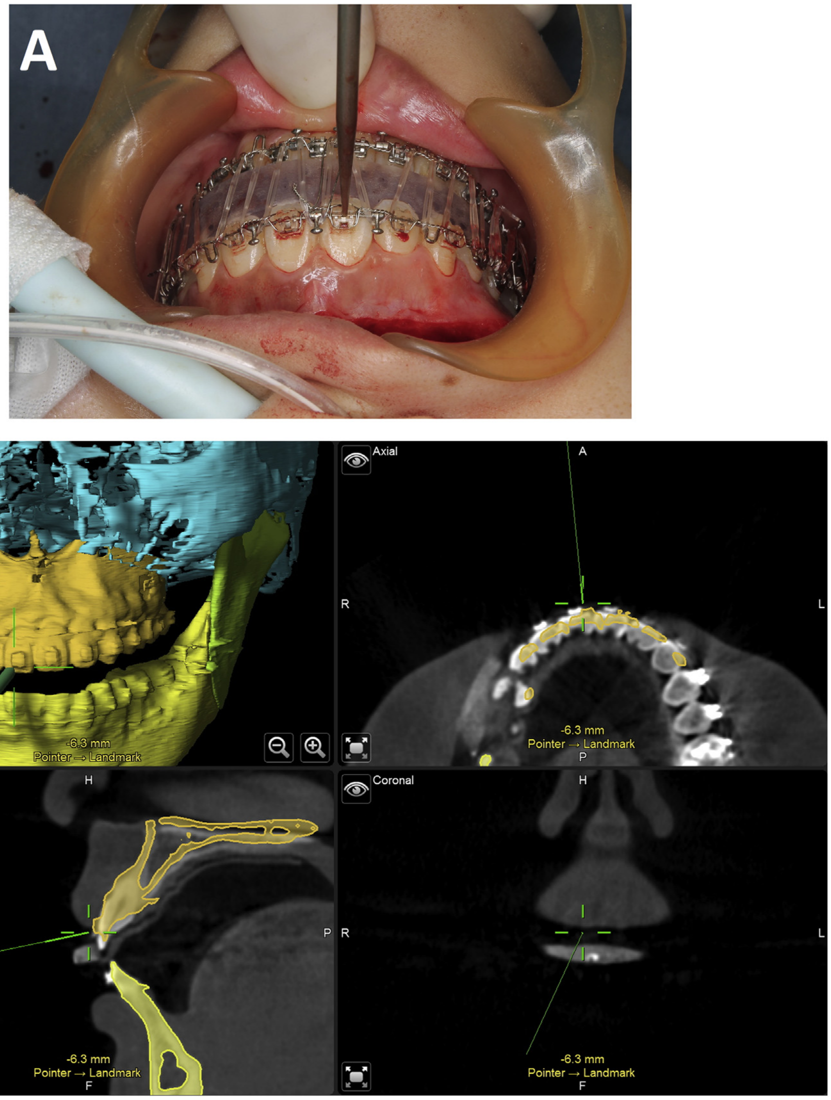

Fig. 5. Movement of the maxillary segment using the CAD/CAM splint: To move the mobile maxillary segment to the planned position, intermaxillary fixation is applied through a CAD/CAM splint (A). The image after movement of the maxillary segment is displayed on the navigation system screen, and the bracket of the central incisor is indicated using the pointer, confirming movement of this point to the position coinciding with that on the simulation image (B).

preoperative 3D skull image and predicted postoperative image created by surgical simulation, and a preoperative 3D skull image and postoperative 3D skull image were superimposed, respectively. To evaluate the accuracy of maxillary positioning in Le Fort I osteotomy, measurement points were set to the following 6 points: anterior nasal spine (ANS), mesio-incisal angle of the right maxillary central incisor, cusp tips of bilateral maxillary canines, and mesiobuccal cusp tips of bilateral maxillary first molars. Distances between each measurement point set on the preoperative CBCT image and simulated prediction image were measured on the X, Y and Z axes. In addition, the result was defined as the predicted movement distance (PMD) at each measurement point. Similarly, distances between each measurement point set on pre- and postoperative CBCT images were measured, and the result was defined as the actual movement distance (AMD) at each measurement point. The difference between the PMD and AMD for each measurement point was calculated (PMD-AMD), and this absolute value was considered as the accuracy of positioning of the maxillary segment. A measurer other than the operator measured points twice during a 7-day interval, and the mean rounded to the third decimal place was adopted as the measured value (Fig. 6).

2.9. *Statistical analysis*

To evaluate measurement accuracy, the significance of differences between first and second measured values on the X, Y, and Z axes was analyzed at each measurement point using the Wilcoxon signed-rank test. In addition, measurement error on each axis was calculated using the Dahlberg formula [8] ($Se^2 = \Sigma d^2/2n$; where Se is measurement error, d is difference between first and second measured values, and n is number of subjects).

The Wilcoxon signed-rank test was used to examine the significance of differences between the distance on the estimated image and postoperative CBCT on each axis. In addition, the Wilcoxon signed-rank test was also used to examine the significance of differences between linear distance on the estimated image and that on the postoperative CBCT image in 3D space. Specifically, we first calculated these distances for both images as $\sqrt{\Delta x^2 + \Delta y^2 + \Delta z^2}$, where Δx, Δy and Δz are the movement distances along corresponding axes, then used these linear distances to examine the significance of differences.

Whether the error between predicted and postoperative CT images differed significantly among measurement points was analyzed on each axis using Scheffe's multiple comparison test. Statistical analysis was

Fig. 6. Superimposition between the image predicted by the simulation and postoperative CT images: The postoperative image predicted by preoperative simulation and 3D skeletal image of the head prepared from CBCT images acquired after surgery are superimposed, enabling analysis of errors between models by comparison of measured values.

performed using R version 3.50, setting the level of significance at less than 5%.

In order to interpret the results of accuracy of maxillary segment positioning, the authors considered the positional planned and post-operative outcomes of smaller than 2 mm to be clinically insignificant [9, 10, 11].

3. Results

Subjects comprised 24 females and 11 males, ranging in age from 17–45 years (mean, 26.7 years). The underlying deformity was mandibular prognathism in 9 patients, bimaxillary protrusion in 4, facial asymmetry in 9, prognathism and asymmetry in 4, anterior open bite in 5, bilateral cleft lip and palate in 3, and left cleft lip and palate in 1, for 35 patients in total (Table 1). Surgical simulation and design of the CAD/CAM splint were performed by surgeons. According to the protocol of the present study, the patient visited the clinic twice for dental arch impression taking and CBCT to fabricate the intermediate splint for repositioning. The patient's dental plaster model was scanned using a 3D scanner, and the data were imported into ProPlan, simulation software for orthognathic surgery. Surgical simulation was performed and a splint was designed. The process of importing the data into the navigation system through coordinate transformation software took approximately 45 min. The data for the splint designed using simulation software were sent to the 3D printer in the dental laboratory with internet access, and the splint was fabricated.

In order to investigate the influence of the present protocol on the surgical time, the surgical time using the present protocol was compared with that for 35 surgical cases performed by the same surgeons between January and December 2013. The subjects comprised 26 females and 9 males, ranging in age from 18 to 60 years (mean age, 28.7 years). Significant differences were analyzed using the t-test. The surgical time for two-jaw surgery was 218.6 $\pm$ 47.3 (mean $\pm$ SD) min using the conventional method and 253.2 $\pm$ 51.3 min using the present protocol. The surgical time was extended by 34.6 min with the present protocol ($p = 0.00$).

PMD and AMD at each measurement point measured on the X, Y and Z axes were compared between first and second measurements using the Wilcoxon signed-rank test, and no significant differences were detected. Measurement errors of PMD calculated by the Dahlberg formula were less than 0.71 mm on the X axis, 1.02 mm on the Y axis, and 0.60 mm on the Z axis. Measurement errors of AMD were less than 0.78 mm on the X axis, 1.21 mm on the Y axis, and 0.61 mm on the Z axis (Table 2).

PMD at each measurement point by superimposing the preoperative 3D skull image and postoperative prediction image simulated by surgical simulation was a maximum of 3.75 mm and a minimum of −2.79 on the X axis, a maximum of 6.27 mm and a minimum of −4.11 mm on the Y axis, and a maximum of 7.30 mm and a minimum of −3.28 mm in the Z axis. AMD at each measurement point by superimposing pre- and post-operative 3D skull images was a maximum of 3.84 mm and a minimum of −3.21 mm on the X axis, a maximum of 7.08 mm and a minimum of −4.72 mm on the Y axis, and a maximum of 6.41 mm and a minimum of −3.54 mm on the Z axis. Mean error between PMD and AMD (PMD-AMD) at each measurement point on the 3 axes was a maximum of 0.78 mm and a minimum of 0.57 mm on the X axis, a maximum of 1.03 mm and a minimum of 0.64 mm in the Y axis, and a maximum of 0.90 mm and a minimum of 0.84 mm in the Z axis. The Wilcoxon signed rank test was conducted to compare predicted and actual movement at each measurement point on the X, Y and Z axes, showing no significant differences at most measurement points on the X and Y axes, but significant differences at all points on the Z axis (Table 3).

No difference between linear distance on the estimated image and postoperative CBCT was seen for most points in 3D space (Table 4).

Whether errors between predicted and postoperative CT images on the X, Y and Z axes differed significantly among measurement points was analyzed using Scheffe's multiple comparison test. No measurement point-associated significant differences were noted (Table 5).

Table 1
Patient information.

Case	Age (yr)	Sex	Diagnosis	Treatment plan for maxilla
1	21	M	BCLP	Advancement
2	21	M	BCLP	Advancement
3	45	F	Bimaxillary protrusion	Set-back, impaction
4	23	F	Prognathism	Impaction, clockwise-rotation
5	26	F	Prognathism	Impaction, clockwise-rotation
6	24	M	BCLP	Advancement, right shift, impaction
7	43	F	Prognathism	Impaction, clockwise-rotation
8	25	F	Prognathism and facial asymmetry	Right shift, impaction
9	22	F	Prognathism	Impaction
10	29	F	Facial asymmetry	Left shift, impaction
11	20	M	Prognathism	Impaction, clockwise-rotation
12	19	F	Anterior open bite	Impaction
13	17	F	Facial asymmetry	Advancement, left shift
14	23	F	Bimaxillary protrusion	Set-back, impaction
15	24	F	Facial asymmetry	Advancement, right shift, impaction
16	22	F	Bimaxillary protrusion	Impaction, clockwise-rotation
17	25	F	Anterior open bite	Impaction, clockwise-rotation
18	32	M	Prognathism	Advancement
19	21	M	Prognathism	Advancement, impaction
20	42	M	Prognathism and facial asymmetry	Yaw rotation, impaction
21	39	F	Anterior open bite	Impaction, clockwise-rotation
22	32	F	Prognathism and facial asymmetry	Yaw rotation, left up
23	28	F	Prognathism and facial asymmetry	Right shift, left up
24	20	F	Prognathism	Left shift, impaction
25	20	F	Facial asymmetry	Right shift, right up, yaw rotation
26	20	F	Facial asymmetry	Set-back, impaction
27	23	F	Facial asymmetry	Right up, yaw rotation
28	29	M	Bimaxillary protrusion	Set-back, impaction
29	20	F	Facial asymmetry	Posterior impaction, right shift
30	24	M	Anterior open bite	Posterior impaction,
31	23	F	Facial asymmetry	Advancement, right up
32	41	F	Facial asymmetry	Setback, impaction
33	38	F	Anterior open bite	Impaction, clockwise-rotation
34	36	M	Prognathism	Advancement, left shift
35	18	M	Left CLP	Advancement

F, female; M, male; CLP, cleft lip and plate; BCLP, bilateral cleft lip and palate.

4. Discussion

An intermediate splint for maxillary repositioning has recently been reported as unnecessary, because the maxillary segment can be moved with high accuracy using a navigation system in two-jaw surgery [12, 13, 14]. However, to accurately place the maxillary segment mobilized by Le Fort I osteotomy to the position determined by preoperative simulation, the segment needs to be placed so as to merge several measurement points on the actual maxillary segment with those on the predicted maxilla. Repositioning of the maxillary segment pattern in two-jaw surgery is not limited to simple advancement, and varies depending on the case, potentially including backward movement, impaction of the molar region by clockwise rotation, correction of the occlusal plane, and yawing rotation. When the repositioning pattern is complex, processes such as removal of bone interfering with the mobile maxillary segment and repeated confirmation of the position of the mobile maxillary segment are needed, making the difficulty level vary among patients. Moreover, the mobile maxillary segment is unstable and readily moves, and is inevitably loaded with force due to mini-plate fixation. Fixing the maxillary segment by moving the maxilla according to surgical simulation may thus be difficult when confirming the position using navigation alone while maintaining the 3D positional relationship at high accuracy. Preparation of a mobile maxillary segment-repositioning guide using CAD/CAM and placement of the maxilla without setting the baseline to the mandible have recently been tried as a method to reflect the results of simulation in actual surgery [15, 16, 17]. However, this complicates the surgical procedure, such as limiting the mini plate position for fixation of the maxillary segment and/or greater surgical invasion than strictly necessary. Accurate movement of the maxillary segment to the simulated position was considered possible using surgical simulation by moving the maxillary segment with the CAD/CAM splint, and subsequently confirming that the moved position matched the simulated position using surgical navigation in Le Fort I osteotomy. In the present study, the accuracy of maxillary segment positioning was investigated by comparing the maxillary segment position moved during this procedure and the position simulated by surgical simulation in patients requiring two-jaw surgery.

Table 2
Measurement error (ME) and significant differences between first and second measured values of movement distances on each axis.

	X axis		Y axis		Z axis	
	ME (mm)	*p*-value	ME (mm)	*p*-value	ME (mm)	*p*-value
Predicted movement distance (PMD)						
Point 1	0.71	0.658	0.65	0.719	0.48	0.510
Point 2	0.52	0.064	0.50	0.857	0.27	0.957
Point 3	0.52	0.034	0.52	0.441	0.35	0.451
Point 4	0.57	0.725	0.50	0.112	0.28	0.446
Point 5	0.50	0.600	0.74	0.898	0.29	0.137
Point 6	0.54	0.918	1.02	0.909	0.60	0.915
Actual movement distance (AMD)						
Point 1	0.70	0.850	0.58	0.521	0.61	0.474
Point 2	0.43	0.051	0.46	0.550	0.51	0.533
Point 3	0.56	0.036	0.66	0.481	0.45	0.137
Point 4	0.78	0.723	0.51	0.588	0.41	0.238
Point 5	0.63	0.452	0.70	0.067	0.41	0.800
Point 6	0.56	0.600	1.21	0.193	0.49	0.338

Point 1, ANS; Point 2, mesio-incisal angle of the right maxillary central incisor; Point 3, cusp tip of the right maxillary canine; Point 4, cusp tip of the left maxillary canine; Point 5, mesiobuccal cusp tip of the maxillary right first molar; Point 6, mesiobuccal cusp tip of the maxillary left first molar.

To confirm whether the maxillary segment can be placed during surgery as simulated using the CAD/CAM-fabricated splint, the data adopted for splint design in surgical simulation are required for navigation during surgery. However, no navigation system equipped with simulation software containing a CAD/CAM-fabricated splint-designing function has yet been developed. On the other hand, simulation software designed exclusively for craniomaxillofacial surgery, ProPlan CMF version 3.0, can simulate orthognathic surgery and design intermediate splints in consideration of the occlusal relationship, but is incompatible with the simulation software of the navigation system, iPlan CMF 3.0. To use STL data from the surgical simulation prepared using ProPlan CMF version 3.0 with the navigation system, the coordinates of the ProPlan CMF version 3.0 STL data were converted to those of iPlan 3.0 using coordinate transformation software and employed during navigation-assisted surgery, enabling maxillary repositioning using the splint prepared by CAD/CAM and comparison of the maxillary position with simulation results in real time using navigation.

To investigate errors of maxillary position between simulation and actual surgeries, the preoperative simulation image and postoperative 3D-CT image were superimposed. Statistical analyses showed no difference between preoperative 3D simulation and actual result in any direction. When the error between preoperative simulation and actual surgery is within 2 mm, the accuracy of the operation is considered high.

Table 3
Comparison of predicted movement distance (PMD) and actual movement distance (AMD) on the 3 axes at each point.

	PMD (mm)			AMD (mm)			PMD-AMD (mm)	
	Mean ± SD	Min	Max	Mean ± SD	Min	Max	Mean ± SD	p-value
X axis (horizontal direction)								
Point 1	−0.15 ± 1.28	−2.56	2.04	−0.21 ± 1.38	−2.95	2.83	0.57 ± 0.55	0.608
Point 2	−0.07 ± 1.40	−2.79	3.37	−0.13 ± 1.15	−2.02	3.70	0.77 ± 0.62	0.716
Point 3	0.00 ± 1.21	−2.57	2.28	−0.20 ± 1.14	−2.08	3.05	0.74 ± 0.60	0.195
Point 4	0.02 ± 1.30	−2.57	2.60	0.13 ± 1.01	−1.45	2.94	0.78 ± 0.54	0.523
Point 5	0.03 ± 1.41	−2.46	3.39	−0.23 ± 1.35	−2.92	2.86	0.64 ± 0.45	0.030
Point 6	0.13 ± 1.56	−2.72	3.75	0.13 ± 1.40	−3.21	3.84	0.57 ± 0.56	0.716
Y axis (anteroposterior direction)								
Point 1	0.93 ± 2.04	−2.79	6.27	0.84 ± 2.00	−3.16	5.22	0.64 ± 0.53	0.368
Point 2	0.57 ± 2.19	−2.82	5.66	0.86 ± 2.10	−3.46	4.90	1.03 ± 0.73	0.166
Point 3	0.61 ± 2.14	−2.52	4.91	0.64 ± 2.14	−3.10	5.68	0.70 ± 0.56	0.878
Point 4	0.44 ± 2.12	−3.60	5.53	0.57 ± 2.12	−3.57	4.31	0.97 ± 0.67	0.502
Point 5	0.86 ± 2.40	−4.11	6.03	0.72 ± 2.34	−3.67	7.08	0.69 ± 0.55	0.481
Point 6	0.59 ± 2.56	−3.92	5.57	0.59 ± 2.37	−4.72	4.62	0.93 ± 0.67	0.918
Z axis (vertical direction)								
Point 1	1.38 ± 1.84	−1.53	6.76	0.99 ± 1.65	−2.63	5.29	0.90 ± 0.63	0.032
Point 2	0.88 ± 1.75	−1.93	6.98	0.30 ± 1.75	−1.64	6.09	0.89 ± 0.66	0.000
Point 3	1.14 ± 1.92	−1.28	6.60	0.56 ± 1.76	−2.45	6.41	0.96 ± 0.75	0.004
Point 4	1.12 ± 1.60	−0.92	5.81	0.68 ± 1.53	−2.35	4.28	0.89 ± 0.62	0.003
Point 5	1.68 ± 2.31	−2.35	7.30	1.14 ± 2.07	−2.45	5.48	0.86 ± 0.70	0.001
Point 6	1.66 ± 1.73	−3.28	4.63	1.10 ± 1.67	−3.54	5.05	0.84 ± 0.65	0.001

Point 1, ANS; Point 2, mesio-incisal angle of the right maxillary central incisor; Point 3, cusp tip of the right maxillary canine; Point 4, cusp tip of the left maxillary canine; Point 5, mesiobuccal cusp tip of the maxillary right first molar; Point 6, mesiobuccal cusp tip of the maxillary left first molar.

Table 4
Comparison of linear distances on the estimated image and on the postoperative CBCT image in 3D space at each point.

	PMD (mm)			AMD (mm)			PMD-AMD (mm)	
	Mean ± SD	Min	Max	Mean ± SD	Min	Max	Mean ± SD	p-value
Point 1	3.06 ± 1.57	0.74	7.18	2.81 ± 1.52	0.62	5.93	0.73 ± 0.64	0.174
Point 2	2.83 ± 1.65	0.27	8.03	2.67 ± 1.52	0.69	7.35	0.92 ± 0.69	0.522
Point 3	2.87 ± 1.73	0.21	7.68	2.68 ± 1.54	0.66	8.67	0.91 ± 0.71	0.461
Point 4	2.81 ± 1.50	0.24	6.71	2.63 ± 1.24	0.58	5.19	0.91 ± 0.57	0.302
Point 5	3.53 ± 1.97	0.07	8.34	3.20 ± 1.72	0.61	9.14	0.94 ± 0.70	0.058
Point 6	3.51 ± 1.59	0.23	5.86	3.12 ± 1.41	0.75	6.23	0.93 ± 0.61	0.029

Point 1, ANS; Point 2, mesio-incisal angle of the right maxillary central incisor; Point 3, cusp tip of the right maxillary canine; Point 4, cusp tip of the left maxillary canine; Point 5, mesiobuccal cusp tip of the maxillary right first molar; Point 6, mesiobuccal cusp tip of the maxillary left first molar.

Mean error at the 6 measurement points was ≤1.03 mm on the 3 axes, suggesting that simulation results accurately reflected the conditions of actual surgery. Absence of a significant difference in measured values among most measurement points suggested that confirmation of the position at one measurement point is sufficient for maxillary repositioning using a CAD/CAM-fabricated splint. Based on the above findings, the method of moving the maxilla mobilized by Le Fort I osteotomy using a CAD/CAM-fabricated splint and confirming its position using navigation may be useful to accurately reflect the results of surgical simulation in actual surgery.

The accuracy of this surgery was investigated by superimposing the model of the postoperative skull as predicted by simulation on the 3D skeletal model constructed from CBCT data acquired after surgery. For superimposition of the two models, a software algorithm equipped in iPlan CMF 3.0 was used, using random landmarks on the image as benchmarks. Positions of these 2 CT images coincided, showing high accuracy. The accuracy of measurement is influenced by the accuracy of the pre- and postoperative 3D-CBCT models. Da Silva et al. [18] measured the error between linear distance in an axial CBCT image and the actual value using a phantom (diameter, 5 cm; length, 10 cm; and a 1-mm ditch), and observed the superior accuracy of distance measurements in the axial direction. Patcas et al. [19] imaged autopsied bodies using CBCT and CT, and analyzed the error of the distance from the cutting edge to the alveolar crest between the actual measurement and measurement on the image. They stated that the error was 0.14 mm on CBCT, lower than that on CT (0.23 mm), and accuracy of the distance measured on a reconstruction image prepared from CBCT images was very high. Although the objective of the above studies was not the accuracy of the 3D model, measurement accuracy was higher for CBCT than for CT, so accuracy of the 3D model using such data may have been relatively high.

The reference antenna-fixing methods include direct fixation to the skull and fixation using a head band. Direct fixation to the skull is very invasive for patients undergoing orthognathic surgery, and they experience a strong sense of resistance. We thus selected fixation with a head band. A slight change in reference antenna position results in a large error in the accuracy of navigation. In orthognathic surgery in which the head presentation has to be changed several times during surgery, accuracy has to be confirmed many times and correction is necessary. With the widely employed laser registration, facial unevenness is scanned utilizing laser reflection and merged with CT data. However, problems have been encountered, such as errors generated by general anesthesia-induced skin shift, and difficulty in evaluation and correction of errors generated during surgery [20, 21, 22]. In the present study, CBCT images were acquired while the patient held a resin splint with 5 markers made of X-ray opaque resin in the mouth, and registration was performed considering these markers as basic coordinates. For registration using this method, reference points were easily identified without the influence of artifacts from orthodontic appliances, and registration was able to be repeated many times within 1 min during surgery. Switching to landmark

Table 5
Probability value by Scheffe's multiple comparison test between predicted and postoperative CT images differed significantly among measurement points in the horizontal, anteroposterior, and vertical directions. No measurement point-associated significant differences were noted.

	X axis (horizontal)	Y axis (anteroposterior)	Z axis (vertical)
Point 1 vs Point 2	1.000	0.997	0.060
Point 1 vs Point 3	0.984	1.000	0.737
Point 1 vs Point 4	0.977	1.000	0.947
Point 1 vs Point 5	0.897	1.000	1.000
Point 1 vs Point 6	1.000	1.000	1.000
Point 2 vs Point 3	1.000	0.989	0.769
Point 2 vs Point 4	0.990	1.000	0.451
Point 2 vs Point 5	0.973	1.000	0.142
Point 2 vs Point 6	0.907	0.989	0.051
Point 3 vs Point 4	0.940	1.000	0.997
Point 3 vs Point 5	0.996	1.000	0.897
Point 3 vs Point 6	0.784	1.000	0.704
Point 4 vs Point 5	0.703	1.000	0.992
Point 4 vs Point 6	0.999	1.000	0.993
Point 5 vs Point 6	0.451	0.996	0.999

Point 1, ANS; Point 2, mesio-incisal angle of the right maxillary central incisor; Point 3, cusp tip of the right maxillary canine; Point 4, cusp tip of the left maxillary canine; Point 5, mesiobuccal cusp tip of the maxillary right first molar; Point 6, mesiobuccal cusp tip of the maxillary left first molar.

registration before mobilization of the maxillary segment enabled evaluation and correction of the navigation accuracy many times during surgery, even after mobilization of the maxilla, which was useful to maintain navigation accuracy in orthognathic surgery.

Advantages of the protocol of this study included the the accuracy of maxillary segment repositioning to the position set by simulation was able to be confirmed at a number of measurement points in real time. In addition, the simulation software for orthognathic surgery enables fast and easy surgical simulation for correcting yawing and cant by moving the maxillary segment three-dimensionally. The intermediate splint designed by the simulation software can be fabricated in a shorter time using rapid prototyping technology than using the conventional method. However, as the present surgical plan was developed using simulation based on the skull, changes in the soft tissue by orthognathic surgery cannot be predicted. The ideal skull does not necessarily indicate ideal facial contour results. The relationship between changes in the postoperative skull and postoperative facial contours needs to be elucidated to develop a system that can predict facial contours after orthognathic surgery. Another disadvantage of the present protocol is that include the extension of the surgical time by 34.6 min because registration needed to be repeated several times to set up the navigation and confirm its accuracy. Furthermore, three different software programs, including simulation software for orthognathic surgery, coordinate transformation software, and navigation software, were necessary. If the simulation software supplied with navigation system improves and CAD/CAM splints for maxillary positioning can be designed in the future, the protocol is considered to become more practical. Considering the development of the present simulation software, it is considered to be technically feasible.

In maxillary repositioning during Le Fort I osteotomy, the method of confirming the position of the maxillary segment moved using CAD/CAM splints designed by simulation software is useful for positioning the maxilla to the preoperatively planned position using simulation.

Declarations

Author contribution statement

Tatsuo Shirota: Conceived and designed the experiments; Performed the experiments; Analyzed and interpreted the data; Wrote the paper.

Sunao Shiogama: Analyzed and interpreted the data; Contributed reagents, materials, analysis tools or data.

Yusuke Asama: Performed the experiments; contributed reagents, materials, analysis tools or data.

Motohiro Tanaka: Performed the experiments; Analyzed and interpreted the collected data.

Yuji Kurihara: Performed the experiments; Analyzed and interpreted the collected data.

Hiroshi Ogura: Conceived and designed the experiments; Analyzed and interpreted the data; Wrote the paper.

Takaaki Kamatani: Conceived and designed the experiments; Analyzed and interpreted the data.

Funding statement

This research did not receive any specific grant from funding agencies in the public, commercial, or not-for-profit sectors.

Competing interest statement

The authors declare no conflict of interest.

Additional information

No additional information is available for this paper.

References

[1] E. Ellis 3rd, Bimaxillary surgery using an intermediate splint to position the maxilla, J. Oral Maxillofac. Surg. 57 (1999) 53.
[2] R.R.J. Cousley, M. Bainbridge, P.E. Rossouw, The accuracy of maxillary positioning using digital model planning and 3D printed wafers in bimaxillary orthognathic surgery, J. Orthod. 44 (2017) 256.
[3] E. Shaheen, Y. Sun, R. Jacobs, C. Politis, Three-dimensional printed final occlusal splint for orthognathic surgery: design and validation, Int. J. Oral Maxillofac. Surg. 46 (2017) 67.
[4] F. Vale, J. Scherzberg, J. Cavaleiro, D. Sanz, et al., 3D virtual planning in orthognathic surgery and CAD/CAM surgical splints generation in one patient with craniofacial microsomia: a case report, Dental Press J. Orthod. 21 (2016) 89.
[5] S. Aboul-Hosn Gentenero, F. Hernández-Alfaro, 3D planning in orthognathic surgery: CAD/Cam surgical splints and prediction of the soft and hard tissues results- Our experience in 16 cases, J. Cranio-Maxillo-Fac. Surg. 30 (2011) 1.
[6] F.G. Ritto, A.R.M. Schmitt, T. Pimentel, et al., Comparison of the accuracy of maxillary position between conventional model surgery and virtual surgical planning, Int. J. Oral Maxillofac. Surg. 47 (2018) 160.
[7] P.E. Dawson, A classification system for occlusions that relates maximal intercuspation to the position and condition of the temporomandibular joints, J. Prosthet. Dent 75 (1996) 60–66.
[8] G. Dahlberg, Statistical Methods for Medical and Biological Students, Interscience Publications, New York, 1940, pp. 1–140.
[9] S.S. Hsu, J. Gateno, R.B. Bell, et al., Accuracy of a computer-aided surgical simulation protocol for orthognathic surgery: a prospective multicenter study, J. Oral Maxillofac. Surg. 71 (2013) 128.
[10] N. Zhang, S. Liu, Z. Hu, et al., Accuracy of virtual surgical planning in two-jaw orthognathic surgery: comparison of planned and actual results, Oral Surg. Oral Med. Oral Pathol. Oral Radiol. 122 (2016) 143.
[11] S.J. Chin, F. Wilde, M. Neuhaus, et al., Accuracy of virtual surgical planning of orthognathic surgery with aid of CAD/CAM fabricated surgical splint-A novel 3D analyzing algorithm, J. Cranio-Maxillo-Fac. Surg. 45 (2017) 1962–1970.
[12] M.J. Zinser, R.A. Mischkowski, T. Dreiseidler, et al., Computer-assisted orthognathic surgery: waferless maxillary positioning, versatility, and accuracy of an image-guided visualization display, Br. J. Oral Maxillofac. Surg. 51 (2013) 827.
[13] B. Li, L. Zhang, H. Sun, S.G. Shen, et al., A new method of surgical navigation for orthognathic surgery: optical tracking guided free-hand repositioning of the maxillomandibular complex, J. Craniofac. Surg. 25 (2014) 406.
[14] H.W. Chang, H.H. Lin, P. Chortrakarnkij, et al., Intraoperative navigation for single-splint two-jaw orthognathic surgery: from model to actual surgery, J. Cranio-Maxillo-Fac. Surg. 43 (2015) 111.
[15] M.J. Zinser, R.A. Mischkowski, H.F. Sailer, et al., Computer-assisted orthognathic surgery: feasibility study using multiple CAD/CAM surgical splints, Oral Surg. Oral Med. Oral Pathol. Oral Radiol. 113 (2012) 673.
[16] J.W. Polley, A.A. Figueroa, Orthognathic positioning system: intraoperative system to transfer virtual surgical plan to operating field during orthognathic surgery, J. Oral Maxillofac. Surg. 71 (2013) 911.
[17] M. Heufelder, F. Wilde, S. Pietzka, et al., Clinical accuracy of waferless maxillary positioning using customized surgical guides and patient specific osteosynthesis in bimaxillary orthognathic surgery, J. Cranio-Maxillo-Fac. Surg. 45 (2017) 1578.

[18] N.C. da Silva, M. Barriviera, J.L. Junqueira, et al., Intraobserver and interobserver reproducibility in linear measurements on axial images obtained by cone-beam computed tomography, Imaging Sci. Dent. 47 (2017) 11.
[19] R. Patcas, G. Markic, L. Müller, et al., Accuracy of linear intraoral measurements using cone beam CT and multidetector CT: a tale of two CTs, Dentomaxillofac. Radiol. 41 (2012) 637.
[20] S. Mazzoni, G. Badiali, L. Lancellotti, et al., Simulation-guided navigation: a new approach to improve intraoperative three-dimensional reproducibility during orthognathic surgery, J. Craniofac. Surg. 21 (2010) 1698.
[21] R. Marmulla, J. Mühling, T. Lüth, et al., Physiological shift of facial skin and its influence on the change in precision of computer-assisted surgery, Br. J. Oral Maxillofac. Surg. 44 (2006) 27.
[22] D. Venosta, Y. Sun, F. Matthews, et al., Evaluation of two dental registration-splint techniques for surgical navigation in cranio-maxillofacial surgery, J. Cranio-Maxillo-Fac. Surg. 42 (2013) 448.